

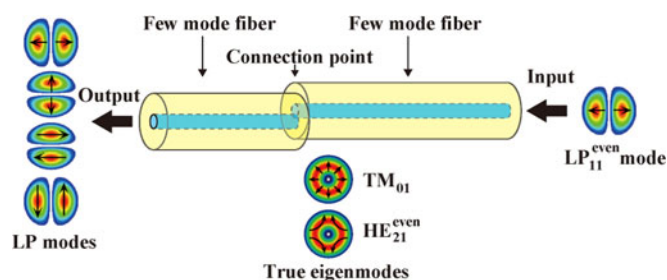
Accurate Analysis of Crosstalk Between LP_{11} Quasi-Degenerate Modes Due to Offset Connection Using True Eigenmodes

Volume 10, Number 1, February 2018

Seiya Miura

Tatsuhiko Watanabe, *Member, IEEE*

Yasuo Kokubun, *Fellow, IEEE*



DOI: 10.1109/JPHOT.2017.2786706

1943-0655 © 2017 IEEE

Accurate Analysis of Crosstalk Between LP₁₁ Quasi-Degenerate Modes Due to Offset Connection Using True Eigenmodes

Seiya Miura ¹, Tatsuhiko Watanabe,^{1,2} *Member, IEEE*,
and Yasuo Kokubun ³, *Fellow, IEEE*

¹Graduate School of Engineering, Yokohama National University, Yokohama
240-8501, Japan

²ETH Zurich Institute of Electromagnetic Fields, Zurich 8092, Switzerland

³Faculty of Engineering, Yokohama National University, Yokohama 240-8501, Japan

DOI:10.1109/JPHOT.2017.2786706

1943-0655 © 2017 IEEE. Personal use is permitted, but republication/redistribution requires IEEE permission. See http://www.ieee.org/publications_standards/publications/rights/index.html for more information.

Manuscript received October 31, 2017; revised December 18, 2017; accepted December 19, 2017. Date of publication December 25, 2017; date of current version February 1, 2018. This work was supported in part by the National Institute of Information and Communications Technology, Japan, under “Research on Innovative Technologies of Amplification, Connection, and Transmission for SDM” and in part by JSPS KAKENHI under Grant 16K14263. Corresponding author: Yasuo Kokubun (e-mail: kokubun-yasuo-sd@ynu.ac.jp).

Abstract: Linearly polarized (LP) modes in few-mode fibers are not true eigenmodes but approximated modes constituting of linear combinations of true eigenmodes. Therefore, the vector field profile in a few-mode fiber must be expressed in terms of the true eigenmodes with complex amplitudes involving a phase difference corresponding to the propagation distance. Owing to this property of LP mode propagation, the propagation characteristics of few-mode fibers cannot be accurately analyzed using conventional LP modes. In this study, the crosstalk between LP₁₁ quasi-degenerate modes due to offset connection is accurately analyzed using matrix formalism expressing the linear combination of true eigenmodes. The difference in the analytical results between the LP modes and the eigenmodes revealed that the propagation of few-mode fibers should be analyzed using true eigenmodes.

Index Terms: Few-mode-fiber, eigenmodes, splicing, offset, crosstalk.

1. Introduction

The traffic in optical transmission networks is increasing year by year, and the transmitted power density in a fiber has also rapidly increased accordingly. The transmission capacity of a single-core single-mode fiber is predicted to be limited to about 100 Tbps due to the nonlinear Shannon limit [1]. Even for short-reach transmission, if the optical power exceeds a certain threshold value, a destructive propagation phenomenon called a fiber fuse occurs, originating from small defects in the core, and the transmission capacity is limited to a certain value. To solve this problem, few-mode fibers (FMFs), in which the number of modes is increased by increasing the core diameter, have been proposed and some experiments on ultra high-capacity transmission have been demonstrated [2].

In these experiments, the LP mode [3] has been widely used to describe the light propagation in an FMF. It is known, however, that an LP mode is no more than an approximated mode and is expressed by a linear combination of true eigenmodes, such as HE, EH, TE and TM modes

TABLE 1
Definition of Degenerate LP Modes


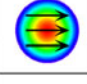
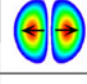
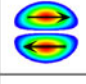
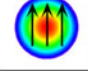
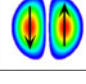
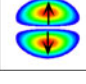
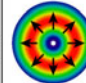
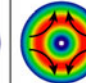
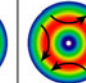
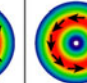
	LP ₀₁	LP ₁₁ ^{even}	LP ₁₁ ^{odd}
x - polarization			
y - polarization			

TABLE 2
Definition of Eigenmodes Corresponding to First Order Mode

	TM ₀₁	HE ₂₁ ^{even}	HE ₂₁ ^{odd}	TE ₀₁
Electric field distribution				

[4]–[7]. Since the light emitted from a laser diode (LD) is linearly polarized, LP modes are naturally excited at the input end of an FMF. However, even if a specific LP₁₁ mode is selectively excited at the input end, the electric field profile transforms its shape along with the propagation in the fiber [8], [10], [11] because there is a small difference in the propagation constants between the true eigenmodes [12], [13]. Therefore, MIMO-DSP has been inevitable in mode-division multiplexing transmission [14].

In addition, since the eigenmodes constituting an LP mode are quasi-degenerate, the propagation characteristics of FMFs have been expressed using the LP mode. Therefore, It has not been reported [15] that some types of analysis based on the LP mode lead to false conclusions. One such incorrect conclusion is that orthogonally polarized LP modes cannot be coupled to each other by an offset connection or by perturbation at the core-cladding boundary.

In this study, the authors analyze the evolution of the field profile of LP₁₁ quasi-degenerate modes in terms of true eigenmodes and show how the coupling between LP₁₁ degenerate modes at a connection point with axial offset can be expressed in terms of true eigenmodes. As a result, it is revealed that propagation characteristics such as the crosstalk due to the offset connection should be analyzed using the eigenmodes not using the LP modes.

2. Analysis of Mode Coupling at Connection Point

2.1 Relation Between LP Modes and True Eigenmodes

The fundamental and first-order LP modes have a linearly polarized electric field as summarized in Table 1.

The electric field profiles of LP₁₁ modes are expressed by a linear combination of two true eigenmodes [5]–[7], and this relation between LP modes and true eigenmodes summarized in Table 2 is expressed by the following matrix [11], [15].

$$\begin{bmatrix} \mathbf{E} (LP_{11-x}^{\text{even}}) \\ \mathbf{E} (LP_{11-y}^{\text{odd}}) \\ \mathbf{E} (LP_{11-x}^{\text{odd}}) \\ \mathbf{E} (LP_{11-y}^{\text{even}}) \end{bmatrix} = \frac{1}{\sqrt{2}} \begin{bmatrix} 1 & -1 & 0 & 0 \\ 1 & 1 & 0 & 0 \\ 0 & 0 & 1 & -1 \\ 0 & 0 & 1 & 1 \end{bmatrix} \cdot \begin{bmatrix} \mathbf{E} (TM_{01}) \\ \mathbf{E} (HE_{21}^{\text{even}}) \\ \mathbf{E} (HE_{21}^{\text{odd}}) \\ \mathbf{E} (TE_{01}) \end{bmatrix}. \quad (1)$$

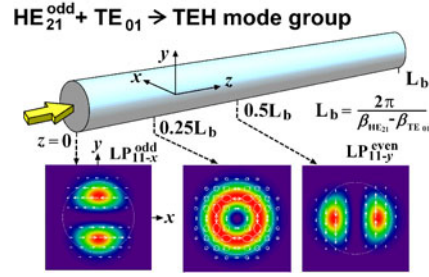


Fig. 1. Evolution of intensity profile and field vector of LP₁₁ modes with propagation distance.

Here the matrix in (1) is denoted as M_1 . This matrix relation can be separated into two 2×2 matrix relations, and the upper 2×2 matrix relation consists of TM_{01} and HE_{21}^{even} modes. This mode group is called the TMH mode group and the other mode group is called the TEH mode group [13].

Using the inverse matrix of M_1 , true eigenmodes can be expressed by a linear combination of two LP modes as follows [11]:

$$\begin{bmatrix} \mathbf{E}(TM_{01}) \\ \mathbf{E}(HE_{21}^{\text{even}}) \\ \mathbf{E}(HE_{21}^{\text{odd}}) \\ \mathbf{E}(TE_{01}) \end{bmatrix} = \frac{1}{\sqrt{2}} \begin{bmatrix} 1 & 1 & 0 & 0 \\ -1 & 1 & 0 & 0 \\ 0 & 0 & 1 & 1 \\ 0 & 0 & -1 & 1 \end{bmatrix} \cdot \begin{bmatrix} \mathbf{E}(LP_{11-x}^{\text{even}}) \\ \mathbf{E}(LP_{11-y}^{\text{odd}}) \\ \mathbf{E}(LP_{11-x}^{\text{odd}}) \\ \mathbf{E}(LP_{11-y}^{\text{even}}) \end{bmatrix}. \quad (2)$$

Here the matrix in (2) is denoted as M_1^{-1} because this is the inverse matrix of M_1 .

2.2 Phase Difference Between Eigenmodes Due to Propagation

Since the propagation constants of true eigenmodes are slightly different from each other, even if an LP mode is excited at the input end, the electromagnetic field distribution varies with the propagation distance due to the interference between the constituent true eigenmodes, as predicted theoretically [15] and confirmed experimentally [16]. This interference is illustrated in Fig. 1 [11].

If the output eigenmodes are expressed in terms of the input eigenmodes, the following relations can be separately obtained for the TMH and TEH mode groups:

$$\begin{bmatrix} \mathbf{E}(TM_{01}) \\ \mathbf{E}(HE_{21}^{\text{even}}) \end{bmatrix}_{\text{output}} = \frac{e^{-j\beta_{aM} \cdot z}}{\sqrt{2}} \begin{bmatrix} e^{j\Delta\phi_M} & 0 \\ 0 & e^{-j\Delta\phi_M} \end{bmatrix} \cdot \begin{bmatrix} \mathbf{E}(TM_{01}) \\ \mathbf{E}(HE_{21}^{\text{even}}) \end{bmatrix}_{\text{input}}, \quad (3)$$

$$\begin{bmatrix} \mathbf{E}(HE_{21}^{\text{odd}}) \\ \mathbf{E}(TE_{01}) \end{bmatrix}_{\text{output}} = \frac{e^{-j\beta_{aE} \cdot z}}{\sqrt{2}} \begin{bmatrix} e^{j\Delta\phi_E} & 0 \\ 0 & e^{-j\Delta\phi_E} \end{bmatrix} \cdot \begin{bmatrix} \mathbf{E}(HE_{21}^{\text{odd}}) \\ \mathbf{E}(TE_{01}) \end{bmatrix}_{\text{input}}, \quad (4)$$

where $\Delta\phi_M$, $\Delta\phi_E$, β_{aM} and β_{aE} are expressed by

$$\Delta\phi_M = \frac{\beta_{HE} - \beta_{TM}}{2} \cdot z = \frac{\Delta\beta_M}{2} \cdot z, \quad (5)$$

$$\Delta\phi_E = \frac{\beta_{HE} - \beta_{TE}}{2} \cdot z = \frac{\Delta\beta_E}{2} \cdot z, \quad (6)$$

$$\beta_{aM} = \frac{\beta_{HE} + \beta_{TM}}{2}, \quad (7)$$

$$\beta_{aE} = \frac{\beta_{HE} + \beta_{TE}}{2}. \quad (8)$$

Here, z is the propagation distance from the input end to the connection point and β_{HE} , β_{TM} , and β_{TE} are the propagation constants of the HE_{21} , TM_{01} , and TE_{01} modes, respectively. The values of $\Delta\beta_M$ and $\Delta\beta_E$ can be analytically calculated for a step-index fiber [13]. If the fiber has a graded-index profile, the propagation constants can be calculated using some numerical mode analysis tools.

The transmission matrix for the true eigenmodes is given by

$$\begin{bmatrix} \mathbf{E}(TM_{01}) \\ \mathbf{E}(HE_{21}^{\text{even}}) \\ \mathbf{E}(HE_{21}^{\text{odd}}) \\ \mathbf{E}(TE_{01}) \end{bmatrix}_{\text{output}} = \begin{bmatrix} e^{-j\beta_{aM} \cdot z} \begin{bmatrix} e^{j\Delta\phi_M} & 0 \\ 0 & e^{-j\Delta\phi_M} \end{bmatrix} & \begin{bmatrix} 0 & 0 \\ 0 & 0 \end{bmatrix} \\ e^{-j\beta_{aE} \cdot z} \begin{bmatrix} e^{-j\Delta\phi_E} & 0 \\ 0 & e^{j\Delta\phi_E} \end{bmatrix} & \begin{bmatrix} 0 & 0 \\ 0 & 0 \end{bmatrix} \end{bmatrix} \cdot \begin{bmatrix} \mathbf{E}(TM_{01}) \\ \mathbf{E}(HE_{21}^{\text{even}}) \\ \mathbf{E}(HE_{21}^{\text{odd}}) \\ \mathbf{E}(TE_{01}) \end{bmatrix}_{\text{input}} \quad (9)$$

Here, the above 4×4 matrix is denoted by matrix M_2 .

Let $\widetilde{LP}_{\mu\nu}$ denote the electromagnetic field distribution of the intermediate state into which the light excited as an $LP_{\mu\nu}$ mode at the input end is transformed by the phase difference between the constituent eigenmodes resulting from the propagation. For the TMH mode group, the $\widetilde{LP}_{11-x}^{\text{even}}$ and $\widetilde{LP}_{11-y}^{\text{odd}}$ modes are expressed in terms of a transmission matrix and true eigenmodes as follows.

$$\begin{bmatrix} \mathbf{E}(\widetilde{LP}_{11-x}^{\text{even}}) \\ \mathbf{E}(\widetilde{LP}_{11-y}^{\text{odd}}) \end{bmatrix} = \frac{e^{-j\beta_{aM} \cdot z}}{\sqrt{2}} \begin{bmatrix} e^{j\Delta\phi_M} & -e^{-j\Delta\phi_M} \\ e^{j\Delta\phi_M} & e^{-j\Delta\phi_M} \end{bmatrix} \cdot \begin{bmatrix} \mathbf{E}(TM_{01}) \\ \mathbf{E}(HE_{21}^{\text{even}}) \end{bmatrix} \quad (10)$$

For the TEH mode group, a similar relation is obtained as follows.

$$\begin{bmatrix} \mathbf{E}(\widetilde{LP}_{11-x}^{\text{odd}}) \\ \mathbf{E}(\widetilde{LP}_{11-y}^{\text{even}}) \end{bmatrix} = \frac{e^{-j\beta_{aE} \cdot z}}{\sqrt{2}} \begin{bmatrix} e^{-j\Delta\phi_E} & -e^{j\Delta\phi_E} \\ e^{-j\Delta\phi_E} & e^{j\Delta\phi_E} \end{bmatrix} \cdot \begin{bmatrix} \mathbf{E}(HE_{21}^{\text{odd}}) \\ \mathbf{E}(TE_{01}) \end{bmatrix} \quad (11)$$

Since $e^{-j\beta_{aM} \cdot z}/\sqrt{2}$ and $e^{-j\beta_{aE} \cdot z}/\sqrt{2}$ are a carrier components, we omit them.

$$\begin{bmatrix} \mathbf{E}(\widetilde{LP}_{11-x}^{\text{even}}) \\ \mathbf{E}(\widetilde{LP}_{11-y}^{\text{odd}}) \\ \mathbf{E}(\widetilde{LP}_{11-x}^{\text{odd}}) \\ \mathbf{E}(\widetilde{LP}_{11-y}^{\text{even}}) \end{bmatrix} = \begin{bmatrix} \cos \Delta\phi_M & j \sin \Delta\phi_M & 0 & 0 \\ j \sin \Delta\phi_M & \cos \Delta\phi_M & 0 & 0 \\ 0 & 0 & \cos \Delta\phi_E & -j \sin \Delta\phi_E \\ 0 & 0 & -j \sin \Delta\phi_E & \cos \Delta\phi_E \end{bmatrix} \cdot \begin{bmatrix} \mathbf{E}(LP_{11-x}^{\text{even}}) \\ \mathbf{E}(LP_{11-y}^{\text{odd}}) \\ \mathbf{E}(LP_{11-x}^{\text{odd}}) \\ \mathbf{E}(LP_{11-y}^{\text{even}}) \end{bmatrix}_{\text{input}} \quad (12)$$

2.3 Calculation of Normalized Coupling Coefficient for True Eigenmodes

In this analysis, it is assumed that identical fibers are connected without angular deviation of the propagation axis. In other words, only the axial offset is assumed at the connection point.

Defining the electric field of the input mode at the connection point by $E^{(1)}(x, y)$ and that of the output mode at the connection point by $E^{(2)}(x, y)$, the normalized coupling coefficient of electric field is expressed by

$$C^E = \frac{|\iint_{-\infty}^{\infty} E^{(1)}(x, y) E^{(2)*}(x, y) dx dy|}{\sqrt{\iint_{-\infty}^{\infty} |E^{(1)}(x, y)|^2 dx dy} \sqrt{\iint_{-\infty}^{\infty} |E^{(2)}(x, y)|^2 dx dy}} \quad (13)$$

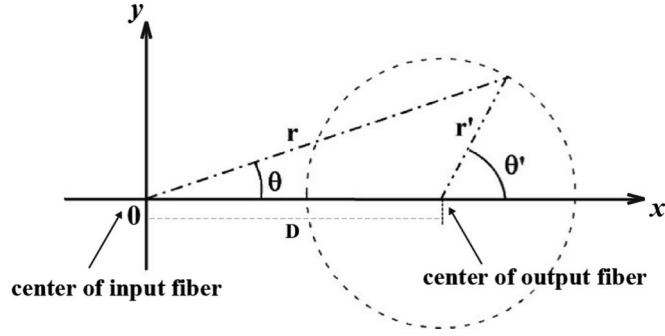


Fig. 2. Coordinate transformation.

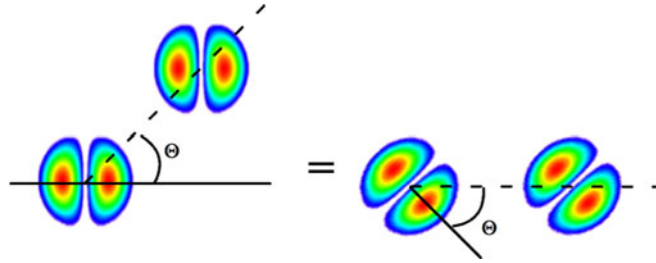


Fig. 3. Conversion of azimuthal angle to take into account angular direction of axial deviation.

Since the optical fiber has circular symmetry, we rewrite (13) in cylindrical coordinates as follows.

$$C^E = \frac{\left| \int_0^{2\pi} \int_0^\infty E^{(1)}(r, \theta) E^{(2)*}(r', \theta') r dr d\theta \right|}{\sqrt{\int_0^{2\pi} \int_0^\infty |E^{(1)}(r, \theta)|^2 r dr d\theta} \sqrt{\int_0^{2\pi} \int_0^\infty |E^{(2)}(r', \theta')|^2 r' dr' d\theta'}} \quad (14)$$

Let us define the axial offset by D . When the coordinates of the input fiber (r, θ) and those of the output fiber (r', θ') are defined as shown in Fig. 2, r' and θ' for the output fiber are represented by r and θ , respectively, as follows.

$$r' = \sqrt{r^2 - 2D \cdot r \cdot \cos \theta + D^2}, \quad (15)$$

$$\theta' = \begin{cases} \theta & (D = 0) \\ \cos^{-1} \left(\frac{r \cdot \cos \theta - D}{r'} \right) & (0 \leq \theta < \pi) \\ -\cos^{-1} \left(\frac{r \cdot \cos \theta - D}{r'} \right) & (\pi \leq \theta < 2\pi), \end{cases} \quad (16)$$

In Fig. 2, the direction of the axial deviation between the input and output fibers connected with the offset is assumed to be in the x direction to simplify the analysis. In the general case, the angular direction of the axial deviation can be expressed by rotating the electric fields of modes as shown in Fig. 3.

Using (15) and (16), the unit vectors $\mathbf{e}_{r'}$ and $\mathbf{e}_{\theta'}$ in the r' and θ' directions are expressed by

$$\mathbf{e}_{r'} = \cos(\theta' - \theta) \mathbf{e}_r + \sin(\theta' - \theta) \mathbf{e}_\theta, \quad (17)$$

$$\mathbf{e}_{\theta'} = \sin(\theta' - \theta) \mathbf{e}_r + \cos(\theta' - \theta) \mathbf{e}_\theta, \quad (18)$$

where \mathbf{e}_r and \mathbf{e}_θ are the unit vectors in the r and θ directions, respectively.

Here, the transverse electric fields of true eigenmodes are expressed in terms of \mathbf{e}_r and \mathbf{e}_θ as follows.

$$\mathbf{E}_t (HE_{21}^{\text{even}}) = \begin{cases} \left[\frac{\beta}{\kappa} \cdot J_1(\kappa r) \cdot \cos(2\theta) \right] \mathbf{e}_r + \left[-\frac{\beta}{\kappa} \cdot J_1(\kappa r) \cdot \sin(2\theta) \right] \mathbf{e}_\theta & |r| \leq a \\ \left[\frac{\beta}{\kappa} \cdot \frac{J_1(\kappa a)}{K_1(\gamma a)} \cdot K_1(\gamma r) \cdot \cos(2\theta) \right] \mathbf{e}_r + \left[-\frac{\beta}{\kappa} \cdot \frac{J_1(\kappa a)}{K_1(\gamma a)} \cdot K_1(\gamma r) \cdot \sin(2\theta) \right] \mathbf{e}_\theta & a < |r|, \end{cases} \quad (19)$$

$$\mathbf{E}_t (HE_{21}^{\text{odd}}) = \begin{cases} \left[\frac{\beta}{\kappa} \cdot J_1(\kappa r) \cdot \sin(2\theta) \right] \mathbf{e}_r + \left[\frac{\beta}{\kappa} \cdot J_1(\kappa r) \cdot \cos(2\theta) \right] \mathbf{e}_\theta & |r| \leq a \\ \left[\frac{\beta}{\kappa} \cdot \frac{J_1(\kappa a)}{K_1(\gamma a)} \cdot K_1(\gamma r) \cdot \sin(2\theta) \right] \mathbf{e}_r + \left[\frac{\beta}{\kappa} \cdot \frac{J_1(\kappa a)}{K_1(\gamma a)} \cdot K_1(\gamma r) \cdot \cos(2\theta) \right] \mathbf{e}_\theta & a < |r|, \end{cases} \quad (20)$$

$$\mathbf{E}_t (TM_{01}) = \begin{cases} \left[\frac{\beta}{\kappa} \cdot J_1(\kappa r) \right] \mathbf{e}_r & |r| \leq a \\ \left[\frac{\beta}{\kappa} \cdot \frac{J_1(\kappa a)}{K_1(\gamma a)} \cdot K_1(\gamma r) \right] \mathbf{e}_r & a < |r|, \end{cases} \quad (21)$$

$$\mathbf{E}_t (TE_{01}) = \begin{cases} \left[\frac{\beta}{\kappa} \cdot J_1(\kappa r) \right] \mathbf{e}_\theta & |r| \leq a \\ \left[\frac{\beta}{\kappa} \cdot \frac{J_1(\kappa a)}{K_1(\gamma a)} \cdot K_1(\gamma r) \right] \mathbf{e}_\theta & a < |r|, \end{cases} \quad (22)$$

where $J_\nu(x)$ and $K_\nu(x)$ and the Bessel function and modified Bessel function of ν -th order, respectively, $\kappa \left(= \sqrt{k_0^2 n_1^2 - \beta^2} \right)$ and $\gamma \left(= \sqrt{\beta^2 - k_0^2 n_2^2} \right)$ are the transverse propagation constants in the core and the cladding, respectively, and a is the core radius. These electric fields are the expressions for the case without an axial offset. When the angle of the axial offset is designated as Θ , the coordinate θ should be replaced by $\theta - \Theta$ instead of θ .

Substituting (19)–(22) into (14) and using (15)–(18), the field coupling coefficients between true eigenmodes can be calculated. The normalized coupling coefficients can be expressed by a matrix form as follows:

$$\begin{bmatrix} \mathbf{E} (TM_{01}) \\ \mathbf{E} (HE_{21}^{\text{even}}) \\ \mathbf{E} (HE_{21}^{\text{odd}}) \\ \mathbf{E} (TE_{01}) \end{bmatrix} = \begin{bmatrix} C_{(TM, TM)}^E & C_{(TM, HE^e)}^E & C_{(TM, HE^o)}^E & C_{(TM, TE)}^E \\ C_{(TM, HE^e)}^E & C_{(HE^e, HE^e)}^E & C_{(HE^e, HE^o)}^E & C_{(HE^e, TE)}^E \\ C_{(TM, HE^o)}^E & C_{(HE^e, HE^o)}^E & C_{(HE^o, HE^o)}^E & C_{(HE^o, TE)}^E \\ C_{(TM, TE)}^E & C_{(HE^e, TE)}^E & C_{(HE^o, TE)}^E & C_{(TE, TE)}^E \end{bmatrix} \begin{bmatrix} \mathbf{E} (TM_{01}) \\ \mathbf{E} (HE_{21}^{\text{even}}) \\ \mathbf{E} (HE_{21}^{\text{odd}}) \\ \mathbf{E} (TE_{01}) \end{bmatrix}, \quad (23)$$

where the subscript (μ, ν) represents the normalized field coupling coefficient between the μ th and ν th modes.

Using the cylindrical symmetry of the structure, (23) can be reduced to

$$\begin{bmatrix} \mathbf{E} (TM_{01}) \\ \mathbf{E} (HE_{21}^{\text{even}}) \\ \mathbf{E} (HE_{21}^{\text{odd}}) \\ \mathbf{E} (TE_{01}) \end{bmatrix} = \begin{bmatrix} P & Q & R & 0 \\ Q & P & 0 & -R \\ R & 0 & P & Q \\ 0 & -R & Q & P \end{bmatrix} \begin{bmatrix} \mathbf{E} (TM_{01}) \\ \mathbf{E} (HE_{21}^{\text{even}}) \\ \mathbf{E} (HE_{21}^{\text{odd}}) \\ \mathbf{E} (TE_{01}) \end{bmatrix}. \quad (24)$$

This 4×4 matrix is denoted as M_3 .

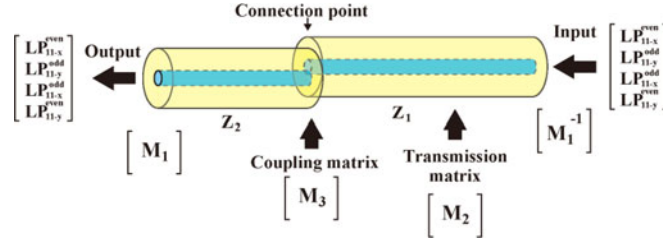


Fig. 4. Order of matrix product.

The formulas used to calculate these coupling coefficients are given by the following equations.

$$P = \frac{\int_0^{2\pi} \int_0^a J_1(\kappa r) J_1(\kappa r') \cos(\theta' - \theta) r dr d\theta}{\int_0^{2\pi} \int_0^a |J_1(\kappa r)|^2 r dr d\theta}, \quad (25)$$

$$Q = \frac{\int_0^{2\pi} \int_0^a J_1(\kappa r) J_1(\kappa r') [\cos\{2(\theta - \Theta)\} \cos(\theta' - \theta) - \sin\{2(\theta - \Theta)\} \sin(\theta' - \theta)] r dr d\theta}{\int_0^{2\pi} \int_0^a |J_1(\kappa r)|^2 r dr d\theta}, \quad (26)$$

$$R = \frac{\int_0^{2\pi} \int_0^a J_1(\kappa r) J_1(\kappa r') [\sin\{2(\theta - \Theta)\} \cos(\theta' - \theta) - \cos\{2(\theta - \Theta)\} \sin(\theta' - \theta)] r dr d\theta}{\int_0^{2\pi} \int_0^a |J_1(\kappa r)|^2 r dr d\theta}, \quad (27)$$

where the terms in the cladding are omitted in (25)–(27) to simplify the representations.

2.4 Crosstalk Between LP₁₁ Modes

Using the above matrices, the overall coupling efficiency can be represented by a single matrix. The equation expressing the coupling efficiency between input LP₁₁ modes and output LP₁₁ modes is given by

$$\begin{bmatrix} E(LP_{11-x}^{\text{even}}) \\ E(LP_{11-y}^{\text{odd}}) \\ E(LP_{11-x}^{\text{odd}}) \\ E(LP_{11-y}^{\text{even}}) \end{bmatrix}_{\text{out}} = \begin{bmatrix} M_1 \\ M_3 \\ M_2 \\ M_1^{-1} \end{bmatrix} \begin{bmatrix} E(LP_{11-x}^{\text{even}}) \\ E(LP_{11-y}^{\text{odd}}) \\ E(LP_{11-x}^{\text{odd}}) \\ E(LP_{11-y}^{\text{even}}) \end{bmatrix}_{\text{in}}, \quad (28)$$

where z_2 is assumed to be zero. Fig. 4 shows the order of the matrix product.

When the matrix relation given by (28) is rewritten as

$$\begin{bmatrix} E(LP_{11x}^{\text{even}}) \\ E(LP_{11y}^{\text{odd}}) \\ E(LP_{11x}^{\text{odd}}) \\ E(LP_{11y}^{\text{even}}) \end{bmatrix}_{\text{out}} = \begin{bmatrix} C_{11} & C_{12} & C_{13} & C_{14} \\ C_{21} & C_{22} & C_{23} & C_{24} \\ C_{31} & C_{32} & C_{33} & C_{34} \\ C_{41} & C_{42} & C_{43} & C_{44} \end{bmatrix} \begin{bmatrix} E(LP_{11x}^{\text{even}}) \\ E(LP_{11y}^{\text{odd}}) \\ E(LP_{11x}^{\text{odd}}) \\ E(LP_{11y}^{\text{even}}) \end{bmatrix}_{\text{in}}, \quad (29)$$

the components of the first row are given by

$$C_{11} = \{P + Q\} \cos \Delta\beta_M \cdot z_1, \quad (30)$$

$$C_{12} = j\{P - Q\} \sin \Delta\beta_M \cdot z_1, \quad (31)$$

$$C_{13} = R \cos \Delta\beta_M \cdot z_1, \quad (32)$$

$$C_{14} = jR \sin \Delta\beta_M \cdot z_1. \quad (33)$$

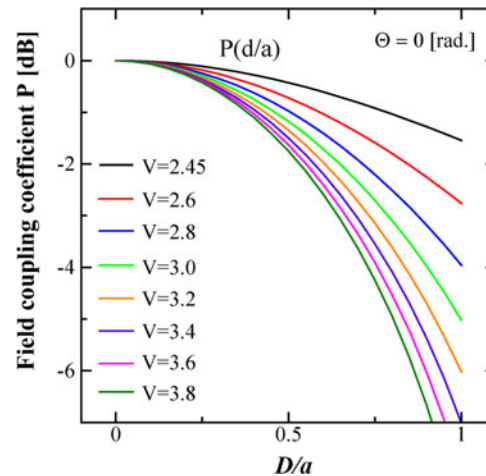


Fig. 5. Dependence of matrix element P on D/a .

The relation between input and output eigenmodes at the connection point is expressed by 4×4 matrix including the axial offset as expressed by (28), and the total propagation is expressed by the product of matrices expressing the coupling at the connection point and the propagation. Since the sinusoidal function with argument $\Delta\beta_M \cdot z$ is involved in these equations, it can be seen that the coupling between two modes whose field vectors are orthogonal to each other occurs at $z_1 \neq 0$, although coupling does not occur at $z_1 = 0$.

Using this matrix representation, the normalized coupling efficiency for the offset connection of an FMF was analyzed.

3. Calculated Results of Coupling Coefficient Between True Eigenmodes

As described in Section 2, the field coupling coefficient between true eigenmodes can be expressed by the matrix in (23). In addition, the 16 matrix components can be reduced to three. Therefore, we analyzed the dependence of the three matrix elements P , Q , and R on the offset distance and azimuth angle using the mathematical tool Mathcad (by PTC).

3.1 Analytical Model of Fiber

In this analysis, we assumed a 2-LP mode fiber which supports LP_{01} and LP_{11} modes.

The relative refractive index difference and the cladding refractive index were assumed to be $\Delta = 0.00375$ and $n_2 = 1.44402$, respectively. The wavelength λ was $1.55 \mu\text{m}$. Assuming a step-index profile, the normalized coupling coefficients P , Q , and R were calculated for various V values in the 2-LP mode region, i.e. $2.405 < V < 3.832$.

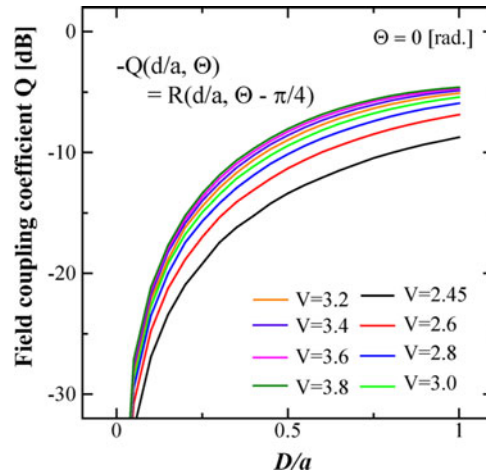
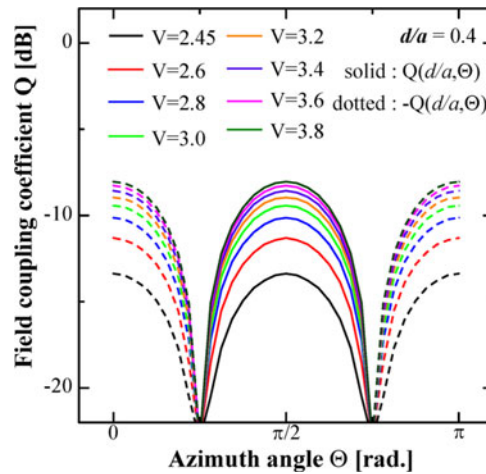
3.2 Matrix Element P

We calculated the values of matrix element P using (25). The result is shown in Fig. 5. It can be easily seen from (25) that P does not depend on the azimuth angle Θ .

Since the matrix element P is the coupling coefficient between the identical mode at the connection point with offset, the value of P decreases with the increase of offset, which corresponds to the increase of connection loss.

3.3 Matrix Elements Q and R

We calculated the matrix elements Q and R using (26) and (27). It is easily seen from (26) and (27) that the matrix elements Q and R depend on the azimuth angle Θ of the direction of offset defined

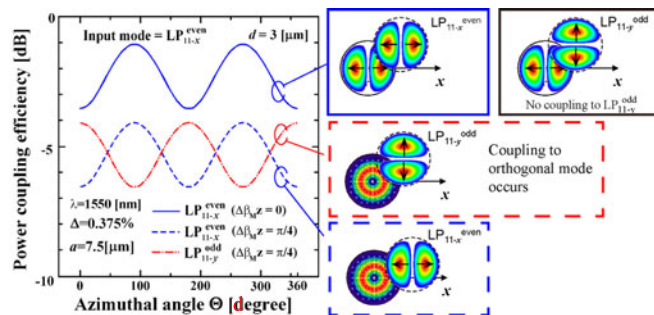
Fig. 6. Dependence of matrix element Q on D/a .Fig. 7. Dependence matrix element Q on Θ .

in Fig. 3. In addition, it is also seen from (26) and (27) that Q and R satisfy the following relation, because (26) and (27) involve sinusoidal terms $\cos\{2(\theta - \Theta)\}$ and $\sin\{2(\theta - \Theta)\}$, respectively.

$$Q(D/a, \theta) = -R\left(D/a, \theta - \frac{\pi}{4}\right) \quad (34)$$

In other words, this relationship is derived from the fact that the HE_{21}^{even} mode and HE_{21}^{odd} mode shown in Table 2 have 45 degrees symmetry while the TM_{01} and TE_{01} modes have no θ dependence. The calculated results are shown in Figs. 6 and 7.

Since the matrix elements Q and R are the coupling coefficients between TM_{01} and HE_{21}^{even} modes and between TE_{01} and HE_{21}^{odd} modes, respectively, the values of these matrix elements are 0 when $D/a = 0$ and increase with the increase of offset as shown in Fig. 6, which means the increase of crosstalk. On the other hand, Q depends on the azimuth angle Θ of the direction of offset as shown in Fig. 7. The Θ dependence of R is obtained by shifting the characteristics shown in Fig. 7 by $\pi/4$.

Fig. 8. Coupling efficiency of LP₁₁ modes.

4. Coupling Coefficient Between LP₁₁ Modes

Using (28), the power coupling efficiency due to an offset connection was calculated for the case of LP_{11-x}^{even} mode incidence using (29)–(33). The power coupling efficiency is calculated by

$$C_{\mu\nu}^P = |C_{\mu\nu}|^2, \quad (35)$$

where μ and ν are the mode labels of output and input modes, respectively. For example, we calculated the power coupling efficiencies and the results are shown in Fig. 8. In this figure, the blue solid line shows the coupling efficiency from the LP_{11-x}^{even} mode to the LP_{11-x}^{even} mode when the phase difference $\Delta\beta_M \cdot z = 0$, which corresponds to the case that the offset occurs at the input end of the few mode fiber and the length of the fiber is much shorter than the beat length of interference between true eigenmodes, as in the case of [8]. The blue dashed line and red dashed line show the power coupling efficiencies from the LP_{11-x}^{even} mode to the LP_{11-x}^{even} mode and to the LP_{11-y}^{odd} mode, respectively, when the phase difference is $\Delta\beta_M \cdot z = \pi/4$ or its odd multiples. When the phase difference is $\Delta\beta_M \cdot z_1 = 0$, coupling occurs from the LP_{11-x}^{even} mode to the LP_{11-x}^{even} mode and there is no coupling between the LP_{11-x}^{even} and LP_{11-y}^{odd} modes because the polarization directions of these two modes are orthogonal as shown in the right upper inset of Fig. 8. This case corresponds to the conventional analysis in which the difference in the propagation constants between true eigenmodes are ignored and the incident LP mode is assumed to propagate to the exit without any change of electromagnetic field. This also corresponds to the case that the offset occurs at the input end of the few mode fiber and the length of the fiber is much shorter than the beat length of the interference between true eigenmodes, like 5cm [8]. The coupling also occurs from the LP_{11-x}^{even} mode to the LP_{11-y}^{odd} mode, but the power coupling efficiency is quite small (≤ -20 dB) because the axis of symmetry is orthogonal for these two modes.

On the other hand, when the phase difference is $\Delta\beta_M \cdot z_1 = \frac{\pi}{4}$, coupling between the LP_{11-x}^{even} and LP_{11-y}^{odd} modes occurs as shown in the right middle inset of Fig. 8. This is opposite to the result of the analysis using LP modes. Since the beat length of the interference between the true eigenmodes constituting an LP mode ranges from several tens centimeters (TEH mode group) to several meters (TMH mode group) [15], the coupling between orthogonal LP modes with orthogonal polarizations occurs at the connection point when the fiber length to the connection point is longer than several meters. As seen from Fig. 8, the crosstalk due to the offset connection occurs between modes with orthogonal polarizations when the propagation distance is not equal to $z = \frac{2N\pi}{\Delta\beta_M}$ or $z = \frac{2N\pi}{\Delta\beta_E}$ where N is an integer. Therefore, the propagation characteristics of FMFs should be analyzed using true eigenmodes not using LP modes.

Although LP₁₁ modes are used as an example of the calculation of connection crosstalk as in the above analysis, the conclusion that the true eigenmodes should be used instead of LP modes is valid for higher order modes. This is because the matrix relation between LP modes and true

eigenmodes is given by

$$\begin{bmatrix} E(L P_{\mu m-x}^{\text{even}}) \\ E(L P_{\mu m-y}^{\text{odd}}) \\ E(L P_{\mu m-x}^{\text{odd}}) \\ E(L P_{\mu m-y}^{\text{even}}) \end{bmatrix} = \begin{bmatrix} 1 & -1 & 0 & 0 \\ 1 & 1 & 0 & 0 \\ 0 & 0 & 1 & -1 \\ 0 & 0 & 1 & 1 \end{bmatrix} \cdot \begin{bmatrix} E(EH_{\mu-1,m}^{\text{even}}) \\ E(HE_{\mu+1,m}^{\text{even}}) \\ E(HE_{\mu+1,m}^{\text{odd}}) \\ E(EH_{\mu-1,m}^{\text{odd}}) \end{bmatrix} \quad (36)$$

and the difference in propagation constants between true eigenmodes also exists for higher order modes. The matrix term in (36) is the same as that in (1).

5. Conclusion

We have analyzed the evolution of the field profile of LP₁₁ quasi-degenerate modes in terms of exact eigenmodes and shown how the coupling between LP₁₁ quasi-degenerate modes at the connection point with the axial offset can be expressed in terms of exact eigenmodes. As a result, it was revealed that the propagation characteristics such as the crosstalk due to the offset connection should be analyzed using the true eigenmodes not using the LP modes. The difference of crosstalk analyses between the LP mode based and true eigenmode based models is that the difference of propagation constants between true eigenmodes is taken into account or not. However, when the mode mixing occurs between true eigenmodes, both analyses based on the true eigenmode and the LP mode can't be effective to calculate the crosstalk correctly. Since some experimental results show that the mode mixing (mode conversion) doesn't occur when the fiber length is shorter than 1 km [9], [16], the crosstalk analysis using true eigenmodes is considered to be effective for the case that the distance to the connection point is shorter than 1 km.

References

- [1] A. D. Ellis, J. Zhao, and D. Cotter, "Approaching the non-linear Shannon limit," *J. Lightw. Technol.*, vol. 28, no. 4, pp. 423–433, Feb. 2010.
- [2] D. Soma *et al.*, "2.05 Peta-bit/s super-Nyquist-WDM SDM transmission using 9.8-km 6-mode 19-core fiber in full C band," in *Proc. Eur. Conf. Opt. Commun.*, Valencia, Spain, 2015, Paper PDP3–2.
- [3] D. Gloge, "Weakly guiding fibers," *Appl. Opt.*, vol. 10, no. 10, pp. 2252–2258, 1971.
- [4] E. Snitzer, "Cylindrical dielectric waveguide modes," *J. Opt. Soc. Amer.*, vol. 51, no. 5, pp. 491–498, May 1961.
- [5] E. Snitzer and H. Osterberg, "Observed dielectrics waveguide modes in the visible spectrum," *J. Opt. Soc. Amer.*, vol. 51, no. 5, pp. 499–505, May 1961.
- [6] A. W. Snyder and J. D. Love, *Optical Waveguide Theory*. London, U.K.: Chapman & Hall, 1983, sec. 14–7.
- [7] A. Sharma, "Constructing linear combinations of LP modes to obtain zeroth order vector modes of optical fibers," *Appl. Opt.*, vol. 27, no. 13, pp. 2647–2649, Jul. 1988.
- [8] J. von Hoyningen-Huene, R. Ryf, and P. Winzer, "LCoS-based mode shaper for few-mode fiber," *Opt. Exp.*, vol. 21, no. 15, pp. 18097–18110, Jul. 2013.
- [9] K. Igarashi, D. Souma, T. Tsuritani, and I. Morita, "Performance evaluation of selective mode conversion based on phase plates for a 10-mode fiber," *Opt. Exp.*, vol. 22, no. 17, pp. 20881–20893, Aug. 2014.
- [10] M. Travagnin, F. Sartori, and M. Ruzzier, "Mode beating analysis by sample stretching and wavelength sweeping in a few-mode fiber," *J. Lightw. Technol.*, vol. 32, no. 3, pp. 494–504, Feb. 2014.
- [11] Y. Kokubun, T. Watanabe, S. Miura, and R. Kawata, "What is a mode in few mode fibers?: Proposal of MIMO-free mode division multiplexing using true eigenmodes," *IEICE Electron. Exp.*, vol. 13, no. 18, pp. 1–12, 2016.
- [12] A. Snyder and W. Young, "Modes of optical waveguides," *J. Opt. Soc. Amer.*, vol. 68, no. 3, pp. 297–309, Mar. 1978.
- [13] H. Kogelnik and P. J. Winzer, "Modal birefringence in weakly guiding fibers," *J. Lightw. Technol.*, vol. 30, no. 14, pp. 2240–2245, Jul. 2012.
- [14] D. Soma *et al.*, "10.16 Peta-bit/s dense SDM/WDM transmission over low-DMD 6-mode 19-core fibre across C + L band," in *Proc. Eur. Conf. Opt. Commun.*, Gothenburg, Sweden, Sep. 17–21, 2017, Paper Th.PDPA.1.
- [15] Y. Kokubun, S. Miura, and T. Watanabe, "Accurate analysis of crosstalk between LP₁₁ degenerate modes due to offset connection using exact eigen-modes," in *Proc. 21st Optoelectron. Conf./Int. Conf. Photon. Switching*, Niigata, Japan, Jul. 3–7, 2016, Paper MC1–1.
- [16] T. Yamaguchi, S. Miura, and Y. Kokubun, "Observation of eigenmode propagation in few-mode fibers by selective LP mode excitation," in *Proc. 22nd Microopt. Conf.*, Tokyo, Japan, Nov. 21, 2017, pp. 7–12.